Laser Physics, Vol. 12, No. 1, 2002, pp. 57–70.

Quantum Deflection of Ultracold Atoms from Mirrors

V. V. Dodonov* and M. A. Andreata

Departamento de Física, Universidade Federal de São Carlos, Via Washington Luiz, km 235, São Carlos, SP, 13565-905 Brasil

e-mail: vdodonov@df.ufscar.br; pmauro@df.ufscar.br

Received July 4, 2001

Abstract—We study the effect of deflection of narrow quantum wave packets from atomic mirrors. If the initial mean value of the momentum is less than the momentum uncertainty, then the mean value of the momentum gradually increases with time at the expense of the energy of quantum fluctuations, due to the effective quantum nonlocal interaction with the boundary, so that essential part (more than half) of the energy of quantum fluctuations can be transformed into the kinetic energy of the center of the wave packet. The evolution of different kinds of packets is analyzed in detail in the case of a free motion in a half-space confined with an ideal impenetrable boundary (including the coordinate and momentum probability distributions, the Wigner quasiprobability, the invariant uncertainty product, etc.). For arbitrary mirrors (totally reflecting or partially transparent) we have obtained general expressions describing the asymptotical behavior of initial narrow packets. A possibility of the verification of the effect in experiments with light ultracold atoms is discussed.

1. INTRODUCTION

Due to impressive achievements in experiments with ultracold atoms demonstrated during last decade [1–9], it becomes possible nowadays (or in the nearest future) to study in laboratories quantum phenomena related to the evolution of wave packets describing the motion of the centers of mass of individual atoms (their "external" degrees of freedom). In particular, many interesting effects can be observed in the case of reflection of cold atoms from some kinds of "atomic mirrors," caused by the interaction of the *internal degrees of freedom* with the gradients of electromagnetic fields in the "evanescent mirrors" [10–14] or "magnetic mirrors" [15, 16]. For not very cold atoms, the motion of the center of mass in these experiments can be considered as classical. However, diminishing the atomic velocity, we inevitably enter the genuine quantum region, and some theoretical studies in this field have been done already [17].

We would like to draw an attention to an interesting effect of the *quantum deflection* [18] of ultracold particles from mirrors. Suppose that one throws a particle in the direction parallel to the surface of some impenetrable wall. If it were a classical particle, it would not "feel" the presence of the wall at all. However, the situation is different in the quantum case, due to the "wave" properties of the "particle," which is represented by some "wave packet." It is well known that the packet rapidly spreads, so in some interval of time it will reach the boundary, and eventually all its plane-wave components will be reflected back. As a consequence, the particle will be deflected from its initial direction of motion. What is the most impressive, it is the fact that the deflection angle can be made arbitrarily large, depending on the initial velocity and the initial transverse uncertainty of the particle position, and, moreover, that it *does not depend on the initial distance* from the boundary, which could be quite macroscopical (say, 10 cm, whereas the initial spread of the packet in the transverse direction could be of the order of 10^{-5} cm). This means that the quantum particle "feels" the wall, even when it passes initially very far from it, in the region free of any force. In a wide sense, this is an analogue of the famous Aharonov–Bohm effect, when a charged particle is deflected by the localized magnetic flux, although it travels through the region where there is no magnetic field. Both phenomena have the same origin: quantum nonlocality and the existence of "wave properties" of quantum objects.

To give a quantitative description, consider the evolution of the mean position and the mean momentum,

$$\langle \hat{x} \rangle \equiv \int \psi^* \hat{x} \psi \, dx, \quad \langle \hat{p} \rangle \equiv -i\hbar \int \psi^* (\partial \psi / \partial x) dx,$$

in the direction x perpendicular to the wall, remembering that the motions in the x and z (along the surface) directions are independent (therefore the parallel component p_z does not change). Calculating the time derivatives of these quantities with the account of the Schrödinger equation

$$\partial \psi / \partial t = (i\hbar/2m) \partial^2 \psi / \partial x^2, \tag{1}$$

one should remember that the integration is performed over the region $x > 0$, and that the wave function satisfies the boundary condition

$$\psi(0, t) \equiv 0. \tag{2}$$

* On leave from Lebedev Physics Institute and Moscow Institute of Physics and Technology, Russia.

Thus one arrives at the following Ehrenfest equations in the presence of an ideal wall:

$$\frac{d\langle x\rangle}{dt} = \frac{\langle p\rangle}{m}, \quad \frac{d\langle p\rangle}{dt} = \frac{\hbar^2}{2m}\left|\frac{\partial\psi}{\partial x}\right|^2_{x=0} \equiv F_r(t), \quad (3)$$

where $F_r(t)$ can be interpreted as an effective "quantum repulsive force." This force is always positive, so it causes the "center of mass" of the quantum packet to move far from the boundary. In the same way one can obtain the equations of motion for the variances $\sigma_x \equiv \langle\hat{x}^2\rangle - \langle\hat{x}\rangle^2$, $\sigma_p \equiv \langle\hat{p}^2\rangle - \langle\hat{p}\rangle^2$, and $\sigma_{px} \equiv \frac{1}{2}\langle\hat{x}\hat{p} + \hat{p}\hat{x}\rangle - \langle\hat{x}\rangle\langle\hat{p}\rangle$:

$$\dot{\sigma}_x = 2\sigma_{xp}/m, \quad \dot{\sigma}_{xp} = \sigma_p/m - F_r(t)\langle x\rangle,$$
$$\dot{\sigma}_p = -2F_r(t)\langle p\rangle.$$

If $\langle p(0)\rangle = 0$ (the initial mean velocity is parallel to the surface of the wall in the three-dimensional case), then the quantities $F_r(t)$, $\langle x\rangle$ and $\langle p\rangle$ are always nonnegative, and all three (co)variances turn out less than they would be in the case of the free space evolution (for the same initial conditions). This means that the "nonlocal interaction" with the wall makes the packet narrower, both with respect to the momentum and coordinate. Besides, the final mean value of the momentum component in the direction perpendicular to the surface, $\langle p(\infty)\rangle$, is different from its initial zero value. The increase of the kinetic energy of the center of mass of the particle, $E_c = \langle p\rangle^2/(2m)$, is achieved at the expense of the *energy of quantum fluctuations* of the packet, $E_{\rm fluc} = \sigma_p/(2m)$, since the total energy is conserved. The deflection angle equals $\theta_{\rm defl} = \tan^{-1}(\langle p(\infty)\rangle/\langle p_z\rangle)$. It appears that $\langle p(\infty)\rangle$ has the same order of magnitude as the initial momentum dispersion in the transverse direction, $\delta p = \sqrt{\sigma_p(0)}$. Consequently, the effect can be significant if the initial mean value of the momentum in the "parallel" direction, $\langle p_z\rangle$, is comparable with δp.[1] If the particle was localized in the region with the extension s in the direction perpendicular to the wall, then $\delta p \sim \hbar/s$. If $s \sim 10^{-5}$ cm, then $\delta p \sim 10^{-22}$ cm/s, which is equivalent to the velocity $v \sim 1$ m/s for the hydrogen atoms, and $v \sim 1$ cm/s for Cs atoms. Such velocities are typical for the experiments with ultracold atoms. To prepare the initial state with the mean velocity directed along the surface and with a small uncertainty in the transverse position, one could use a long thin "atom waveguide" [9, 20–22], through which atoms could exit some trap where they were preliminary cooled to the necessary low energy.

In our preliminary study [18] we considered the problem of quantum deflection under several restrictions: zero initial mean value of the transverse component of momentum, zero correlation coefficient between the coordinate and momentum in the initial *pure* quantum state, and an ideal sharp wall, equivalent to the boundary condition (2). Here we give a more detailed description, removing all these restrictions and taking into account a possible nonperfect reflectivity of the mirror and the difference between the mirror potential and the ideal wall boundary condition.

The plan of the paper is as follows. In Section 2 we consider the case of an ideal sharp boundary, analyzing *exact* solutions describing the evolution of initial *pure* narrow packets and approximate expressions for the evolution of the initial *Gaussian* density matrix of a mixed quantum state. In Section 3 we obtain the formulas giving the *asymptotical* behavior of the packets for nonabsorbing mirrors described in terms of arbitrary reflection and transmission coefficients. In the final section we discuss the results of the paper, the emerging problems to be solved, and the possibilities of the experimental verification of the effect of "quantum deflection" from atomic mirrors.

2. REFLECTION OF PACKETS FROM AN IMPENETRABLE WALL

2.1. Exact Solutions

We start with the following family of *exact* time-dependent solutions to the Schrödinger equation (1) on the half-line with the boundary condition (2), describing the evolution of localized packets:

$$\psi_\alpha(x,t) = 2\mathcal{N}\left[\frac{m}{\pi\hbar\varepsilon^2(t)}\right]^{1/4} \times \exp\left[\frac{im\dot{\varepsilon}}{2\hbar\varepsilon}x^2 + \frac{\varepsilon^*\alpha^2}{2\varepsilon} - \frac{1}{2}|\alpha|^2\right]\sin\left(\sqrt{2m/\hbar}\,\frac{\alpha x}{\varepsilon}\right), \quad (4)$$

where $\mathcal{N} = [1 - \exp(-2|\alpha|^2)]^{-1/2}$ is the normalization factor, and α is an arbitrary complex parameter. The time dependence is "hidden" in the complex function $\varepsilon(t)$, which is an arbitrary solution to the equation $\ddot{\varepsilon} = 0$, satisfying the constraint $\dot{\varepsilon}\varepsilon^* - \dot{\varepsilon}^*\varepsilon = 2i$:[2]

$$\varepsilon(t) = A + iBt, \quad \mathrm{Re}(BA^*) = 1. \quad (5)$$

[1] Perhaps, this explains why the effect of quantum deflection was not discovered earlier, despite that the problem of reflection of wave packets from boundaries was considered by many authors (for the most recent publications see, e.g., [19] and references therein): in all previous studies, the condition $\langle\hat{p}(0)\rangle \gg \sqrt{\sigma_p(0)}$ was assumed (sometimes implicitly) from the beginning.

[2] The solution (4) is a special case ($g = 0$) of a more general family of solutions, which were found for the first time in [23] for the Schrödinger equation with the "singular oscillator potential" $V(x,t) = m\omega^2(t)x^2/2 + gx^{-2}$. In the generic case $\varepsilon(t)$ satisfies the equation $\ddot{\varepsilon} + \omega^2(t)\varepsilon = 0$.

Let us introduce the pure and imaginary parts of the complex coefficient α as follows,

$$\alpha = \gamma - i\beta, \quad \beta > 0, \tag{6}$$

where γ is a real parameter, and parametrize the function $\varepsilon(t)$ as

$$\varepsilon(t) = b^{-1} + b(i + r)t, \quad -\infty < r < \infty. \tag{7}$$

Positive coefficient b is responsible for the initial width of the wave packet, whereas coefficient β determines the initial position of the center of the packet. We are interested in the case when the center of the packet is initially far from the boundary. This means that $\beta \gg 1$, so that we can neglect small corrections of the order of $\exp[-2(\gamma^2 + \beta^2)]$ in all expressions. In particular, factor $\mathcal{N}(|\alpha|)$ can be replaced by unity. In such a case, the initial coordinate distribution $\mathcal{P}(x, t) = |\psi(x, t)|^2$ is very close to the Gaussian,

$$\mathcal{P}(x, 0) \approx (\pi s^2)^{-1/2} \exp[-(x - x_c)^2/s^2], \tag{8}$$

where the initial distance between the boundary and the center of the packet, x_c, and the packet width, s, are given by the expressions

$$x_c = \beta\sqrt{2\hbar/(mb^2)}, \quad s = \sqrt{\hbar/(mb^2)}. \tag{9}$$

Consequently, $x_c/s = \beta\sqrt{2}$, and the initial mean value of the coordinate is much greater than the initial packet width. Now it is convenient to introduce the dimensionless variables as follows,

$$\tilde{x} = \frac{x}{x_c}, \quad \tilde{p} = \frac{ps}{\hbar}, \quad \tau = \frac{b^2}{\beta}t = \frac{\hbar\sqrt{2}}{msx_c}t. \tag{10}$$

The first-order average values of the momentum and coordinate in state (4) can be written as

$$\langle \tilde{p}(\tau)\rangle = \sqrt{2}\beta_r \operatorname{erfi}\left(\frac{\sqrt{2}\nu(\tau)}{\sqrt{R_\beta(\tau)}}\right) e^{-2(\beta^2+\gamma^2)} + p_0 \operatorname{erf}\left(\frac{\beta\mu(\tau)}{\sqrt{R_\beta(\tau)}}\right), \tag{11}$$

$$\langle \tilde{x}(\tau)\rangle = [\nu(\tau)/\beta] \operatorname{erfi}\left(\frac{\sqrt{2}\nu(\tau)}{\sqrt{R_\beta(\tau)}}\right) e^{-2(\beta^2+\gamma^2)} + [\mu(\tau)/\sqrt{2}] \operatorname{erf}\left(\frac{\beta\mu(\tau)}{\sqrt{R_\beta(\tau)}}\right), \tag{12}$$

where the error function $\operatorname{erf}(z)$ and its modification $\operatorname{erfi}(z)$ are defined as [24]

$$\left.\begin{matrix}\operatorname{erf}(z)\\ \operatorname{erfi}(z)\end{matrix}\right\} = \frac{2}{\sqrt{\pi}}\int_0^z \exp(\mp y^2)\,dy.$$

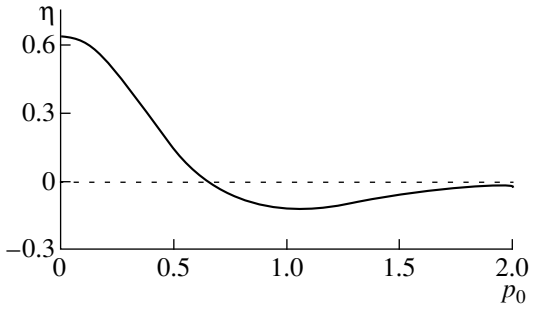

Fig. 1. The momentum transformation coefficient η (21) versus the initial dimensionless average momentum p_0 for $r = 0$.

The other notations are

$$p_0 = \sqrt{2}(\gamma + r\beta), \quad \beta_r = \beta - r\gamma, \tag{13}$$

$$\mu(\tau) = \sqrt{2} + p_0\tau, \quad \nu(\tau) = \beta_r\beta\tau - \gamma, \tag{14}$$

$$R_\beta(\tau) = 1 + 2r\beta\tau + (1 + r^2)(\beta\tau)^2. \tag{15}$$

At the initial moment $\tau = 0$ we have $\langle \tilde{p}(0)\rangle = p_0$ and $\langle \tilde{x}(0)\rangle = 1$, with exponentially small corrections of the order of $\exp(-2\beta^2)$.

The quantity $\langle \tilde{p}^2\rangle$ does not depend on time:

$$\langle \tilde{p}^2\rangle = \frac{1}{2}(1 + r^2) + p_0^2. \tag{16}$$

Other second-order moments depend on time as

$$\langle \tilde{p}\tilde{x} + \tilde{x}\tilde{p}\rangle = 2p_0 + \frac{r}{\beta\sqrt{2}} + \sqrt{2}\tau\langle \tilde{p}^2\rangle, \tag{17}$$

$$\langle \tilde{x}^2\rangle = 1 + \frac{1}{4\beta^2} + \tau\left(\sqrt{2}p_0 + \frac{r}{2\beta}\right) + \frac{\tau^2}{2}\langle \tilde{p}^2\rangle. \tag{18}$$

Using the asymptotical formula [24]

$$\operatorname{erfi}(x \gg 1) \approx (\sqrt{\pi}x)^{-1}\exp(x^2), \tag{19}$$

one can obtain from (11) the asymptotical mean value of the momentum,

$$\langle \tilde{p}(\infty)\rangle = [(1 + r^2)/\pi]^{1/2} \exp\left(-\frac{2p_0^2}{1 + r^2}\right) + p_0 \operatorname{erf}\left(\frac{p_0}{\sqrt{1 + r^2}}\right). \tag{20}$$

The change of the absolute value of the momentum, $\langle \tilde{p}(\infty)\rangle - |\langle \tilde{p}(0)\rangle|$, is maximal for $p_0 = 0$, when the "transformation coefficient" of the average momentum,

$$\eta \equiv [\langle \hat{p}(\infty)\rangle^2 - \langle \hat{p}(0)\rangle^2]/\langle \hat{p}^2\rangle, \tag{21}$$

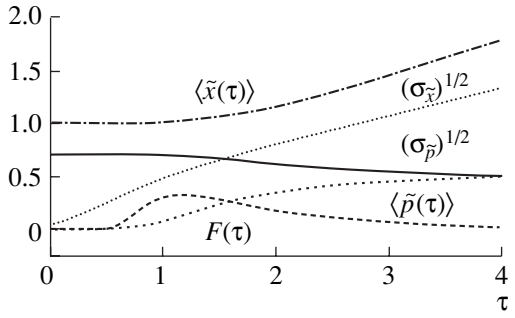

Fig. 2. Evolution of dimensionless mean values of the coordinate and momentum defined in Eq. (10), their mean squared fluctuations, and the dimensionless "quantum repulsive force" (22), versus the dimensionless time τ, for the initial packet (4) with $\beta = 10^4$, $\gamma = r = 0$.

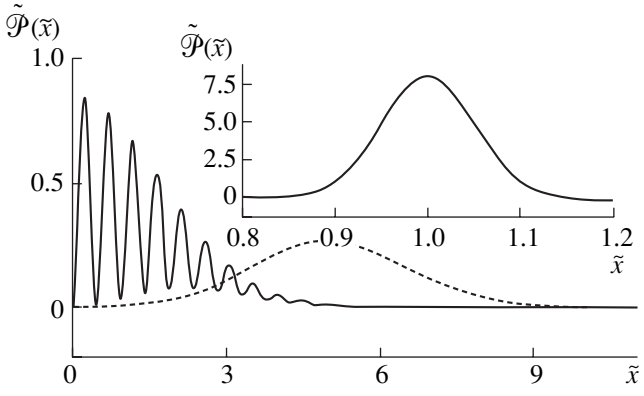

Fig. 3. The coordinate distribution (23) in the case of initial packet (4) with $\beta = 10$ and $r = 0$, for $\tau = 3$ and different values of parameter γ responsible for the initial mean momentum: $\gamma = 0$ (solid line) and $\gamma = -2$ (dashed line). In the insertion we show (in another scale) the initial distribution, which practically does not depend on γ.

equals $\eta = 2/\pi \approx 0.64$. The dependence of the transformation coefficient on the initial average momentum p_0 is shown in Fig. 1 (for $r = 0$). We see that a significant part of the energy of quantum fluctuations is transformed into the energy of the center of mass only for $|p_0| < 0.25$ (note that $\eta(p_0) = \eta(-p_0)$). Moreover, for $|p_0| > 0.7 \approx \sqrt{\sigma_p(0)}$ coefficient η is negative, i.e., the final average momentum appears a little bit less than the initial one. Evidently, these effects are due to the interference between different plane wave components composing the quantum packet. The plots with $r \neq 0$ show the same behavior with respect to the scaled momentum $p_0/\sqrt{1 + r^2}$.

The dimensionless "quantum repulsive force" $\tilde{F} = \beta b^{-3}(m\hbar)^{-1/2}F_r$ is given by

$$\tilde{F} = \frac{4\beta(\gamma^2 + \beta^2)}{\sqrt{\pi}[R_\beta(\tau)]^{3/2}}\exp\left[-\frac{\beta^2\mu^2(\tau)}{R_\beta(\tau)}\right]. \qquad (22)$$

Plots of $\tilde{F}(\tau)$, $\langle\tilde{x}(\tau)\rangle$, $\langle\tilde{p}(\tau)\rangle$, and of mean squared fluctuations of the coordinate and momentum are given in Fig. 2. They show that the particle begins to "feel" the presence of the wall when $\tau > 0.5$. This value agrees, by the order of magnitude, with the time necessary for a quantum packet to spread from its initial dimension s to the value x_c. (Note that the classical particle, for which formally $\hbar = 0$, would never "know" about the boundary.)

The probability density in the position space can be expressed as follows,

$$\tilde{\mathcal{P}}(\tilde{x}, \tau) = \sqrt{\frac{32\beta^2}{\pi R_\beta}}\exp\left(-\frac{\beta^2}{R_\beta}[\mu^2 + 2\tilde{x}^2]\right) \times\left\{\sinh^2\left[\frac{\sqrt{2}\beta^2\mu}{R_\beta}\tilde{x}\right] + \sin^2\left[\frac{2\beta\nu}{R_\beta}\tilde{x}\right]\right\}. \qquad (23)$$

If $\beta\tau \gg 1$, then

$$\tilde{\mathcal{P}}(\tilde{x}, \tau) = \sqrt{\frac{32}{\pi\tau^2(1 + r^2)}}\exp\left(-\frac{\mu^2 + 2\tilde{x}^2}{\tau^2(1 + r^2)}\right) \times\left\{\sinh^2\left[\frac{\sqrt{2}\tilde{x}\mu}{\tau^2(1 + r^2)}\right] + \sin^2\left[\frac{2\beta_r\tilde{x}}{\tau(1 + r^2)}\right]\right\}.$$

If $\tau \gg 1$, the main part of the probability density is concentrated in the region $\tilde{x} \sim \tau$. Then the behavior of $\tilde{\mathcal{P}}(\tilde{x}, \tau)$ depends on the value of the product $p_0\tau$ in function $\mu(\tau)$. If the absolute value of this product is small, then the argument of the $\sinh^2$-function is proportional to τ^{-1}, and one can neglect the contribution of this function. In this case, we have a rapidly oscillating distribution, determined mainly by the $\sin^2$-function, whose argument is proportional to $\beta \gg 1$. On the contrary, if $|p_0\tau| \gg \sqrt{2}$, then the argument of the $\sinh^2$-function practically does not depend on τ for $\tilde{x} \sim \tau$, being proportional to p_0. Consequently, if $|p_0| \gg 1$, then the $\sinh^2$-function is much greater than the $\sin^2$-function, and we have a smooth Gaussian curve without significant oscillations. Such a sensitivity of the long-time probability distribution to the mean value of the initial momentum is shown in Fig. 3, where plots of the position distribution are given for $\beta = 10$ and $\tau = 3$. Even for a not very large absolute mean value of the initial momentum ($\gamma = -2$) we see a broadened and shifted initial Gaussian distribution. At the same time, we see a drastic change in the behavior of the probability density for $p_0 = 0$ and $\beta\tau \gg 1$: it is no more a smooth Gaussian curve (8), but it exhibits strong oscillations, whose spatial period has an order of the initial packet width. For large values of β, the spatial frequency of oscillations is so high, that the plots with $|p_0| \ll 1$ look like some dark regions confined between two envelopes, which corre-

spond to the maximal (1) and minimal (0) values of the $\sin^2$-function.

The *momentum distribution*

$$\mathcal{P}(p,t) = \frac{1}{2\pi\hbar}\left|\int_0^\infty \Psi(x,t)\exp(-ipx/\hbar)dx\right|^2$$

has the form

$$\tilde{\mathcal{P}}(\tilde{p},\tau) = [16\pi(1+r^2)]^{-1/2}\exp\left[-\frac{\tilde{p}^2+p_0^2}{1+r^2}\right] \times\left|\exp\left[-\frac{2\Lambda_\beta v}{R_\beta}\tilde{p}\right]\mathrm{erfc}\left(i\sqrt{\Lambda_\beta}\left[\tilde{p}+\frac{v}{R_\beta}\right]\right)\right. - \left.\exp\left[\frac{2\Lambda_\beta v}{R_\beta}\tilde{p}\right]\mathrm{erfc}\left(i\sqrt{\Lambda_\beta}\left[\tilde{p}-\frac{v}{R_\beta}\right]\right)\right|^2, \quad (24)$$

where

$$2\Lambda_\beta(\tau) = (1-ir)^{-1} + i\beta\tau, \quad (25)$$

$$v(\tau) = \sqrt{2}(\gamma - i\beta)[i\beta\tau(1+ir)-1], \quad (26)$$

and the complementary error function, erfc(z), is defined as [24, 25]

$$\mathrm{erfc}(z) = \frac{2}{\sqrt{\pi}}\int_z^\infty \exp(-y^2)dy \equiv 1 - \mathrm{erf}(z).$$

At $\tau = 0$, the real part of the first erfc-function in Eq. (24) is negative, with very large absolute value, therefore the value of this function is very close to 2 (since $\beta \gg 1$). On the contrary, the second erfc-function is close to $\mathrm{erfc}(+\infty) = 0$. Consequently, the initial momentum distribution is very close (with an exponential accuracy) to the Gaussian,

$$\tilde{\mathcal{P}}(\tilde{p},0) = [\pi(1+r^2)]^{-1/2}\exp\left[-\frac{(\tilde{p}-p_0)^2}{1+r^2}\right].$$

If $\tau \longrightarrow \infty$, the second terms in the arguments of the erfc-functions can be neglected, and the real parts of these arguments tend to $-\infty$ for $p > 0$ and to $+\infty$ for $p < 0$. In the first case each erfc-function tends to 2, whereas in the second case it tends to zero. Consequently, the asymptotical momentum distribution is different from zero only for $p > 0$, being given by the following expression (which does not depend on time):

$$\tilde{\mathcal{P}}_\infty(\tilde{p}) = 2[\pi(1+r^2)]^{-1/2}\exp\left[-\frac{\tilde{p}^2+p_0^2}{1+r^2}\right] \times\left[\cosh\left(\frac{2p_0}{1+r^2}\tilde{p}\right) - \cos\left(\frac{2\sqrt{2}\beta_r}{1+r^2}\tilde{p}\right)\right]. \quad (27)$$

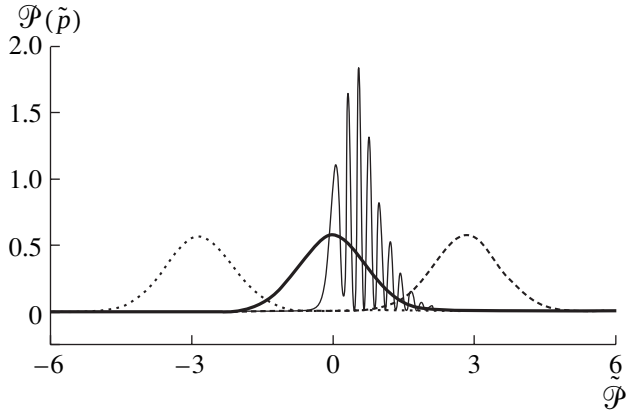

Fig. 4. Evolution of the momentum distribution (24) in the case of initial packet (4) with $\beta = 10$ and $r = 0$, for different values of parameter γ responsible for the initial mean momentum, and for two different instants of the dimensionless time τ. Thick smooth solid curve: $\gamma = 0$, $\tau = 0$; thin oscillating solid curve: $\gamma = 0$, $\tau = 6$; left dotted curve: $\gamma = -2$, $\tau = 0$; right dashed curve: $\gamma = -2$, $\tau = 6$.

Plots of the momentum distribution for $\beta = 10$ are given in Fig. 4. For larger values of β, the period of the momentum density oscillations becomes so small that the plots look like some dark regions between two envelopes. However, these oscillations are significant only for $|p_0| < 1$, i.e., when the initial mean value of the momentum does not exceed the dispersion of the momentum. For larger absolute values of the initial mean momentum, the final distribution is close to the initial one reflected from the axis $p = 0$ (if $p_0 < 0$ and $|p_0| \gg 1$):

$$\tilde{\mathcal{P}}_\infty(\tilde{p}) = [\pi(1+r^2)]^{-1/2}\exp\left[-\frac{(\tilde{p}-|p_0|)^2}{1+r^2}\right].$$

Several plots showing the evolution of the *Wigner function*

$$W(x,p) = 2\int_{-\infty}^{\infty}\Psi^*(x+y)\Psi(x-y)\exp\left(\frac{2ipy}{\hbar}\right)dy$$

for $p_0 = 0$ are given in Fig. 5 (we do not give here the analytical expression, because it is rather cumbersome). One can see how the initial smooth and practically Gaussian distribution is transformed to a highly oscillating quasiprobability distribution, which assumes negative values in many regions of the phase space. This means that the quantum state of the particle becomes essentially "nonclassical." However, for $\tau > 1$ the oscillations are observed only if the initial mean value of the transverse momentum is close to zero, $|p_0| \ll 1$. If $|p_0| > 1$, we have again a smooth quasiprobability distribution without noticeable negative values, which is close to a Gaussian.

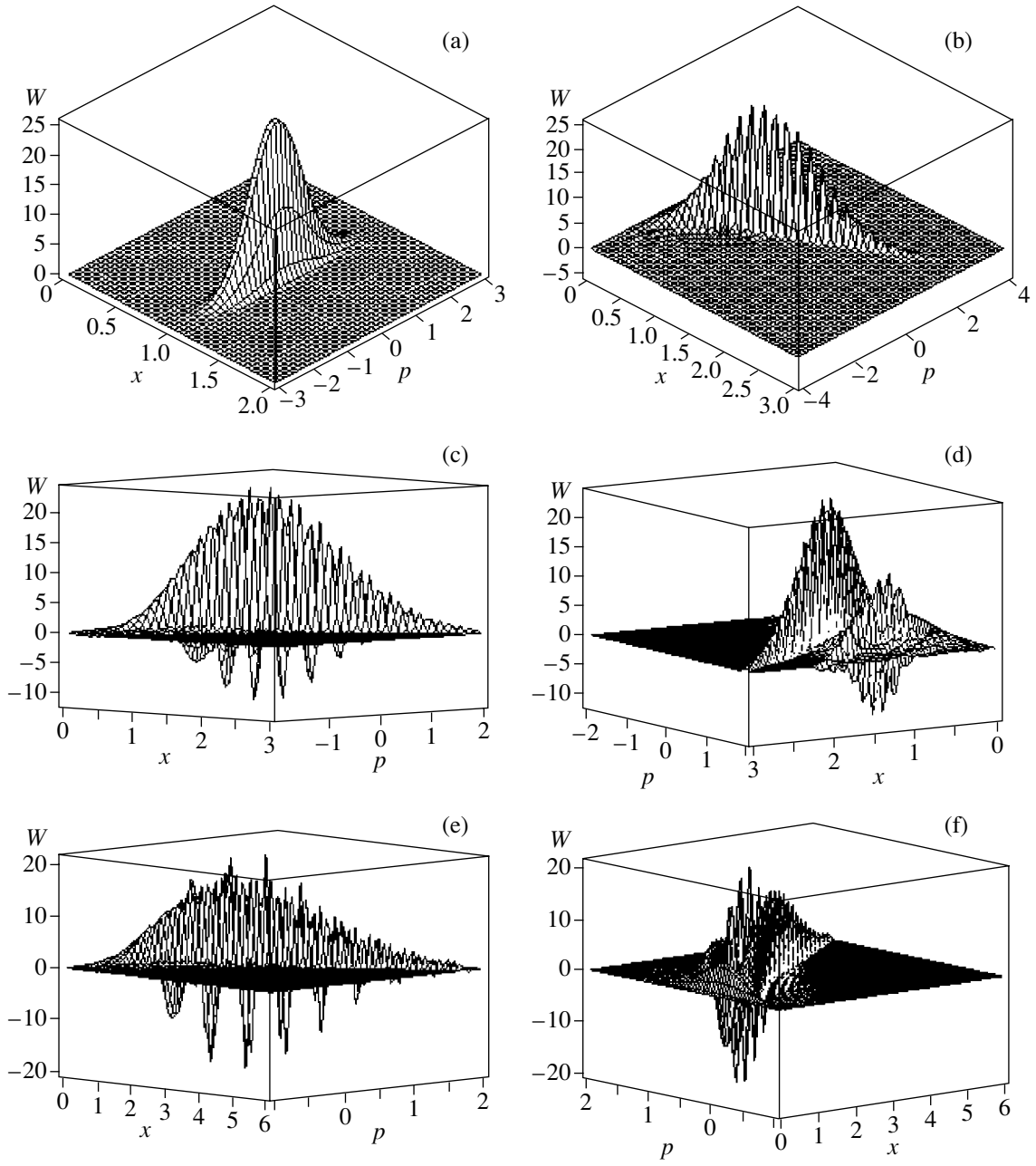

Fig. 5. Evolution of the Wigner function in the case of initial packet (4) with $\beta = 10$ and $r = \gamma = 0$, for different instants of the dimensionless time τ: (a) $\tau = 0$, (b) $\tau = 1$, (c, d) $\tau = 1.5$, (e, f) $\tau = 4$. The pairs (c, d) and (e, f) show the same distributions under different angles, in order to clarify details.

2.2. Evolution of the Invariant Uncertainty Product

Studying the evolution of wave packets, it is a common practice to calculate the "uncertainty product" $\sigma_x\sigma_p$ in order to estimate how close the packet is to the "minimal uncertainty state." For example, a fast growth of this product was interpreted in [26] as an indication to a possibility of a "semiclassical chaos" in quantum systems. As a matter of fact, it is better to use the *invariant uncertainty product* (IUP)

$$\Delta \equiv \sigma_x\sigma_p - \sigma_{xp}^2, \tag{28}$$

which is invariant with respect to arbitrary linear canonical transformations. The product (28) satisfies the Schrödinger–Robertson uncertainty relation $\Delta \geq \hbar^2/4$ [27–30]. Moreover, it does not depend on time for any *quadratic* Hamiltonian with arbitrary time dependent coefficients, being the simplest example of the so

called universal quantum invariants [29, 31, 32]. For non-quadratic Hamiltonians the product (28) can depend on time. It was proposed in [33, 34] to use the rate of change of the function (28) (and of some other similar combinations) to classify the nonlinearities of quantum-mechanical systems.

In the state (4) we have

$$\tilde{\Delta} \equiv \frac{\Delta}{\hbar^2} = \frac{1}{4} + (\beta^2 + \gamma^2)\left\{1 - \mathrm{erf}^2\left(\frac{\beta\mu(\tau)}{\sqrt{R_\beta}}\right)\right.$$
$$\left. - [4(\beta^2 + \gamma^2) + 1]\,\mathrm{erfi}^2\left(\frac{\sqrt{2}\nu(\tau)}{\sqrt{R_\beta}}\right)e^{-4(\beta^2+\gamma^2)}\right\}.$$

If $\beta \gg 1$, as we assume, the value of $\tilde{\Delta}$ remains very close to 1/4 until $\beta\tau \ll 1$, with corrections of the order of $\beta\exp(-2\beta^2)$. The further behavior depends on the sign and the absolute value of the initial mean momentum p_0. If $p_0 < 0$, then a very high maximum is observed at $\tau_m \approx \sqrt{2}/|p_0|$, when the erf-function is close to zero (initially it was very close to 1). With the aid of the asymptotical formula (19) we find for the maximum value of $\tilde{\Delta}$ the following expression:

$$\tilde{\Delta}_{\max} \approx (\beta^2 + \gamma^2)(1 - 2/\pi) \gg 1/4. \qquad (29)$$

For $\tau > \tau_m$ we have a monotonic decrease to the asymptotical value

$$\tilde{\Delta}_\infty \approx \frac{1}{4} + (\beta^2 + \gamma^2)\left\{1 - \mathrm{erf}^2\left(\frac{p_0}{\sqrt{1 + r^2}}\right)\right.$$
$$\left. - \frac{2(\beta^2 + \gamma^2)(1 + r^2)}{\pi\beta_r^2}\exp\left(-\frac{2p_0^2}{1 + r^2}\right)\right\}. \qquad (30)$$

If $p_0 = 0$, then a fast increase of $\tilde{\Delta}$ takes place at $\tau \sim 1$, and after that the IUP eventually goes to the asymptotical maximal value

$$\tilde{\Delta}_\infty^{(0)} = \beta^2(1 + r^2)(1 - 2/\pi) \approx 0.36\beta^2(1 + r^2),$$

which coincides in this case with (29) due to the relation $\gamma = -r\beta$. For positive initial mean momenta, $p_0 > 0$, the evolution of the IUP is monotonic in the whole interval $0 < \tau < \infty$, and the limit value (30) is close again to 1/4 if $p_0 \gg 1$. In Fig. 6, we show the plots of $\tilde{\Delta}$ for $\beta = 10$, $r = 0$, and three values of parameter γ, which correspond to the negative, zero, and positive initial mean momentum p_0.

Parameter r is responsible for the initial correlation between the coordinate and momentum. Defining the *correlation coefficient* as $\mathcal{R} \equiv \sigma_{px}/\sqrt{\sigma_p\sigma_x}$, we have the following expressions for its initial value: $\mathcal{R}(0) = r/\sqrt{1 + r^2}$. Asymptotically $\mathcal{R} \longrightarrow 1$ as $\tau \longrightarrow \infty$ for any value of r. We see that the correlation coefficient plays important role in the evolution of quantum packets. The states with $\mathcal{R} \neq 0$ were named *correlated states* in [28], and they were studied in detail, e.g., in [29, 35–37]. The special case of correlated Gaussian packets in the free space was considered under the name "contractive states" also in [38].

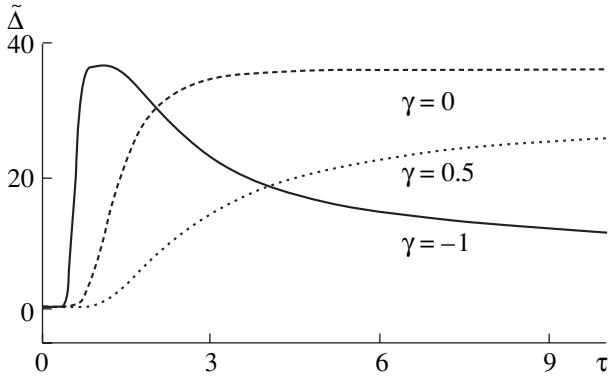

Fig. 6. Evolution of the invariant uncertainty product $\tilde{\Delta} \equiv (\sigma_x\sigma_p - \sigma_{xp}^2)/\hbar^2$, in the case of initial packet (4) with $\beta = 10$ and $r = 0$, for different values of parameter γ responsible for the initial mean momentum.

2.3. Evolution of Gaussian Mixed States

Till now, we considered *pure* quantum states described in terms of the wave function. However, the states created in real experiments hardly are perfectly pure, sooner they are *quantum mixtures* described in terms of the density matrix. To evaluate a possible influence of the impurity of initial states on the effect of quantum deflection, let us consider the simplest case of the initial mixed *Gaussian* state with real parameters (i.e., with zero initial average momentum and zero initial correlation coefficient between the coordinate and momentum):

$$\rho(y, y', 0)$$
$$= \frac{1}{s\sqrt{\pi}}\exp\left\{-\frac{1}{s^2}\left[\frac{y^2 + y'^2}{2(1 - \lambda)} - \frac{\lambda yy'}{1 - \lambda} - x_c(y + y') + x_c^2\right]\right\}, \qquad (31)$$

where s is the initial width of the packet in the coordinate space, x_c is its initial mean position, and parameter λ ($0 \le \lambda < 1$) is responsible for the quantum impurity (which is conserved in time in the absence of dissipation):

$$\mathcal{L} \equiv \mathrm{Tr}\,\hat{\rho}^2 = \sqrt{\frac{1 - \lambda}{1 + \lambda}}.$$

Although function (31) does not satisfy the boundary conditions $\rho(0, y') = \rho(y, 0) = 0$ exactly, an error is exponentially small for $\beta \equiv x_c/(s\sqrt{2}) \gg 1$, being of the order of $\exp(-\beta^2)$, so it can be neglected. The density matrix for $t > 0$ is given by the double integral

$$\rho(x, x', t) = \iint G(x, y, t)G^*(x', y', t)\rho(y, y', 0)dydy', \quad (32)$$

where

$$G(x, y, t) = \left(\frac{m}{2i\pi\hbar t}\right)^{1/2}\left\{\exp\left[-\frac{m(y-x)^2}{2i\hbar t}\right] - \exp\left[-\frac{m(y+x)^2}{2i\hbar t}\right]\right\} \quad (33)$$

is the known propagator for the free motion in the presence of an ideal wall [23, 39–41].

Strictly speaking, the integrals in (32) should be calculated in the interval $0 < y, y' < \infty$, so that the result could be expressed in terms of the error functions. However, since we are interested in the case $\beta \gg 1$, when the initial density matrix is well localized near the point $y = y' = x_c$, we can extend the integrations to the negative semiaxes $-\infty < y, y' < 0$. In this way, we obtain for $\rho(x, x', t)$ a sum of 4 exponential functions. In particular, the diagonal elements read as

$$\rho(\tilde{x}, \tilde{x}, \tau) \approx \sqrt{\frac{8\beta^2}{\pi q(\tau)}}\left\{\exp\left(-\frac{2\beta^2}{q(\tau)}[\tilde{x}^2 + 1]\right) \times \cosh\left[\frac{4\beta^2\tilde{x}}{q(\tau)}\right] - \cos\left[\frac{4\beta^3\tau\tilde{x}}{q(\tau)\mathcal{L}^2}\right] \times \exp\left(-\frac{2\beta^2}{q(\tau)}\left[\frac{\tilde{x}^2}{\mathcal{L}^2} + 1\right]\right)\right\}, \quad (34)$$

where

$$q(\tau) = 1 + \beta^2\tau^2/\mathcal{L}^2,$$

and other notations are the same as in Eq. (10).

For the first- and second-order average values we have

$$\langle\tilde{x}(\tau)\rangle = \left(\frac{q(\tau)}{2\pi\beta^2}\right)^{1/2}[1 - \mathcal{L}^2]\exp\left(-\frac{2\beta^2}{q(\tau)}\right) + \mathrm{erf}\left[\frac{\beta\sqrt{2}}{\sqrt{q}}\right] + \beta\tau\mathcal{L}\,\mathrm{erfi}\left[\frac{\sqrt{2}\beta^2\tau}{\mathcal{L}\sqrt{q}}\right]e^{-2\beta^2},$$

$$\langle\tilde{p}(\tau)\rangle = \frac{\beta\tau}{\sqrt{\pi q(\tau)}}\frac{1-\mathcal{L}^2}{\mathcal{L}^2}\exp\left(-\frac{2\beta^2}{q(\tau)}\right) + \sqrt{2}\beta\mathcal{L}\,\mathrm{erfi}\left[\frac{\sqrt{2}\beta^2\tau}{\mathcal{L}\sqrt{q(\tau)}}\right]\exp(-2\beta^2),$$

$$\langle\tilde{p}^2\rangle = \frac{1}{2\mathcal{L}^2},$$

whereas $\langle\hat{p}\hat{x} + \hat{x}\hat{p}\rangle$ and $\langle\tilde{x}^2\rangle$ are given by Eqs. (17) and (18) with $r = p_0 = 0$. Calculating the asymptotical value $\langle\tilde{p}(\infty)\rangle$, we obtain for the "momentum transformation coefficient" (21) the value $\eta = 2/\pi$, which turns out to be *independent on purity parameter* $\mathcal{L}$. Consequently, a possible quantum impurity does not influence the effect of deflection, at least for initial Gaussian states.

3. REFLECTION OF PACKETS FROM ARBITRARY MIRRORS

For real mirrors, the potential energy is different from the idealized infinitely high sharp potential wall. For example, the "evanescent mirrors" are described by means of the potentials close to $V(x) = V_0\exp(-x/\delta)$ (with some corrections) [17, 42]. In such cases, the detailed evolution of the wave packets can be obtained only in the frameworks of approximate or numerical solutions of the Schrödinger equation. However, the *asymptotical* behavior of the packets (in particular, the "momentum transformation coefficient" (21)) can be calculated practically for any physically reasonable potential.

3.1. Totally Reflecting Mirrors

Let us consider first an arbitrary *totally reflecting* mirror. This means that the potential tends to infinity when $x \longrightarrow -\infty$. If $V(x) = 0$ for $x > 0$, then we have the following complete set of solutions in the semispace $x > 0$:

$$\psi_k(x > 0, t) = \frac{\exp(-ik^2\tilde{t})}{\sqrt{2\pi}}[e^{-ikx} + \chi(k)e^{ikx}], \quad (35)$$

where $k > 0$, $\tilde{t} \equiv \hbar t/(2m)$, and $\chi(k)$ is the amplitude reflection coefficient satisfying the condition $|\chi(k)| = 1$. In the case of an ideal impenetrable wall considered in the preceding section we had $\chi(k) \equiv -1$. If the mirror potential is different from the potential of an infinite wall, then the reflection coefficient depends on the wave number k, because the wave function is different from zero for negative values of x (going to zero as $x \longrightarrow -\infty$), and the phase of $\chi(k)$ is related to the "penetration depth" of the partial plane wave e^{-ikx} before it

will be reflected from the mirror potential. The solutions (35) are normalized as [43]

$$\int \psi_k(x)\psi_{k'}^*(x)dx = \delta(k-k'). \quad (36)$$

The assumption that the motion is free for $x > 0$ is not of principal importance. Actually, (35) is an *asymptotical* form of the solution at $x \longrightarrow \infty$ for any rapidly decaying potential.

Using the formula for the time-dependent propagator of the Schrödinger equation

$$G(x, x'; t, 0) = \int \psi_k(x, t)\psi_k^*(x', 0)dk \quad (37)$$

we obtain the following *exact* expression for $x, x' > 0$:

$$G(x, x'; t, 0) = \int_0^\infty \frac{dk}{2\pi}[e^{ik(x-x')} + e^{-ik(x-x')} + \chi(k)e^{ik(x+x')} + \chi^*(k)e^{-ik(x+x')}]e^{-ik^2\tilde{t}}. \quad (38)$$

We cannot write the propagator for negative values of x or x', without knowledge of the explicit form of the mirror potential and finding the solutions of the Schrödinger equation for $x < 0$. Therefore we cannot calculate the evolution of initial *wide* packets, which were located close to the mirror. Also we cannot follow the evolution of the wave packet when it reaches the mirror. However, considering initial packets which were localized far from the mirror, it is sufficient to know the part of propagator (38) to find the *asymptotical behavior* of the packet, having in mind that as $t \longrightarrow \infty$, only a negligible part of the packet remains in the vicinity of the mirror.[3]

Applying the propagator (38) to a localized initial packet $\psi_0(x')$ one obtains

$$\psi(x, t) = \int_0^\infty \frac{dk}{2\pi}\{e^{ikx}[\varphi_0(k) + \chi(k)\varphi_0(-k)] + e^{-ikx}[\varphi_0(-k) + \chi^*(k)\varphi_0(k)]\}e^{-ik^2\tilde{t}}, \quad (39)$$

where

$$\varphi_0(k) = \int \frac{dx}{\sqrt{2\pi}}\psi_0(x)e^{-ikx} \quad (40)$$

is the initial wave function in the momentum (wave number) representation (the integration can be extended to the whole axis, if $\psi_0(x)$ is localized far from the mirror). If $t \longrightarrow \infty$, the part of the integrand in (39) containing the term $\exp(-ikx - ik^2\tilde{t})$ strongly oscillates, therefore this part "dies out." Consequently, asymptotically the coordinate wave function tends to

$$\psi_{as}(x, t) = \int_0^\infty \frac{dk}{\sqrt{2\pi}}e^{ikx - ik^2\tilde{t}}[\varphi_0(k) + \chi(k)\varphi_0(-k)]. \quad (41)$$

This integral does not go to zero, because its integrand has the stationary point $k_* = x/(2\tilde{t})$. Calculating the Fourier transform of the function (41) one can extend the lower limit of integration over dx to $-\infty$, since the region of localization of the asymptotical wave packet is far to the right from the point $x = 0$. Then one obtains immediately, as in the exact example considered in Section 2, an asymmetrical asymptotical wave function in the momentum representation:

$$\varphi_{as}(k) = \begin{cases} 0, & k < 0 \\ e^{-ik^2\tilde{t}}[\varphi_0(k) + \chi(k)\varphi_0(-k)], & k > 0. \end{cases} \quad (42)$$

If the initial packet is localized near the "central point" x_c, then one can write $\psi_0(x) = \tilde{\psi}_0(x - x_c)$,

$$\varphi_0(k) = \tilde{\varphi}_0(k)\exp(-ikx_c). \quad (43)$$

The asymptotical momentum distribution $\mathcal{P}_{as}(k) = |\varphi_{as}(k)|^2$ equals zero for $k < 0$. For $k > 0$,

$$\mathcal{P}_{as}(k) = |\tilde{\varphi}_0(k)|^2 + |\tilde{\varphi}_0(-k)|^2 + 2\,\mathrm{Re}[\tilde{\varphi}_0^*(k)\tilde{\varphi}_0(-k)\chi(k)e^{2ikx_c}].$$

We see that the concrete form of the function $\chi(k)$ (i.e., the concrete form of the mirror potential) influences only the strongly oscillating part of the asymptotical momentum distribution (the argument of the exponential function kx_c has an order of $x_c/s \gg 1$, where s is the initial characteristic width of the packet in the coordinate space). However, the observable characteristics of the packet, such as the mean momentum or the momentum dispersion, are determined in the asymptotical regime by the average (nonoscillating) distribution

$$\overline{\mathcal{P}}_{as}(k) = \begin{cases} 0, & k < 0 \\ |\tilde{\varphi}_0(k)|^2 + |\tilde{\varphi}_0(-k)|^2, & k > 0, \end{cases} \quad (44)$$

which does not depend on the characteristics of a totally reflecting mirror. In particular,

$$\langle k(0)\rangle = \int_{-\infty}^\infty k|\tilde{\varphi}_0(k)|^2 dk, \quad (45)$$

$$\langle k^2(0)\rangle = \langle k^2(\infty)\rangle = \int_{-\infty}^\infty k^2|\tilde{\varphi}_0(k)|^2 dk, \quad (46)$$

[3] Of course, this implies implicitly some limitations on the admissible forms of the mirror potential, such as an absence of bound states, for example.

$$\langle k(\infty)\rangle = \int_0^\infty k[|\tilde{\varphi}_0(k)|^2 + |\tilde{\varphi}_0(-k)|^2]dk. \quad (47)$$

3.2. Partially Transparent Mirrors

Now let us consider a partially transparent mirror, assuming again for simplicity that its potential is different from zero in a finite domain $-d < x < 0$ (actually, it must decrease rapidly outside this domain). In this case $|\chi(k)| \le 1$, and solution (35) must be continued to the semispace $x < 0$, assuming asymptotically (or for $x < -d$ under our simplified assumptions) the form

$$\psi_k(x, t) = \frac{\zeta(k)}{\sqrt{2\pi}} e^{-ikx - ik^2\tilde{t}}, \quad (48)$$

where $\zeta(k)$ is the *amplitude transmission coefficient* satisfying the condition

$$|\zeta(k)|^2 + |\chi(k)|^2 \equiv 1. \quad (49)$$

Physically, this condition means the absence of absorption in the mirror. Mathematically, it is equivalent to the *unitarity* of evolution. Therefore, we do not consider here absorptive mirrors, because their description requires nonunitary modifications of the Schrödinger equation (although this case may be interesting from the physical point of view). Due to the condition (49), the extended solution preserves the normalization (36). However, now it is insufficient to use only solutions (35) and (48) with $k > 0$. In order to have a complete set of solutions, one has to add the solutions describing the waves coming to the barrier from the left (here $k > 0$):

$$\psi_{-k} = \frac{e^{-ik^2\tilde{t}}}{\sqrt{2\pi}} \begin{cases} e^{ikx} + \chi(-k)e^{-ikx}, & x < 0 \\ \zeta(-k)e^{ikx}, & x > 0. \end{cases}$$

The unitarity condition results in many identities connecting the reflection and transmission coefficients for positive and negative values of k [44, 45]. In particular,

$$\zeta(k) = \zeta(-k), \quad |\chi(k)|^2 = |\chi(-k)|^2, \quad (50)$$

$$\zeta(k)\chi^*(k) + \zeta^*(k)\chi(-k) = 0. \quad (51)$$

The first equality in (50) follows from the reality of the potential, whereas (51) is equivalent to the orthogonality of the states ψ_k and ψ_{-k}.

Now, the integration over dk in the formula for propagator (37) should be performed from $-\infty$ to ∞. However, taking into account the identities (49) and (50), one can verify that the part of the propagator $G_{++}(x, x'; t)$ for positive values of x and x' is given by the same formula (38) as for the totally reflecting mirror, with the only difference that now $\chi(k)$ may be an arbitrary function satisfying the inequality $|\chi(k)| \le 1$. Using the identity (51) one can find also the part of the propagator $G_{-+}(x, x'; t)$ for $x < -d$ and $x' > 0$:

$$G_{-+}(x, x'; t) = \int_0^\infty \frac{dk}{2\pi} e^{-ik^2\tilde{t}}[\zeta(k)e^{-ik(x-x')} + \zeta^*(k)e^{ik(x-x')}].$$

Consequently, the *asymptotical* (for $t \to \infty$) wave function in the momentum representation, for *narrow* initial packets localized far to the right of the mirror, has the following form:

$$\varphi_{as}(k) = \begin{cases} \zeta(k)\tilde{\varphi}_0(k)e^{-ik^2\tilde{t} - ikx_c}, & k < 0 \\ e^{-ik^2\tilde{t}}[\tilde{\varphi}_0(k)e^{-ikx_c} + \chi(k)\tilde{\varphi}_0(-k)e^{ikx_c}], & k > 0. \end{cases} \quad (52)$$

The *averaged* asymptotical momentum distribution reads

$$\overline{\mathcal{P}}_{as}(k) = \begin{cases} |\zeta(k)\tilde{\varphi}_0(k)|^2, & k < 0 \\ |\tilde{\varphi}_0(k)|^2 + |\chi(k)\tilde{\varphi}_0(-k)|^2, & k > 0. \end{cases}$$

Consider, for example, a *symmetrical* initial distribution $\tilde{\varphi}_0(k) = \tilde{\varphi}_0(-k)$, which ensures the zero value of the initial mean momentum. Calculating the mean values in the momentum representation with the aid of the wave function (52), we obtain the following leading terms for $t \to \infty$:

$$\langle x\rangle = \hbar\langle k(\infty)\rangle t/m + x_c\omega,$$

$$\langle x^2\rangle = \hbar^2\langle k^2\rangle t^2/m^2 + x_c^2,$$

$$\langle \hat{x}\hat{p} + \hat{p}\hat{x}\rangle = 2\hbar^2\langle k^2\rangle t/m,$$

where

$$\langle k(\infty)\rangle = 2\int_0^\infty k|\chi(k)|^2|\tilde{\varphi}_0(k)|^2 dk,$$

$$\langle k^2\rangle = 2\int_0^\infty k^2|\tilde{\varphi}_0(k)|^2 dk,$$

$$\omega = 2\int_0^\infty |\zeta(k)|^2|\tilde{\varphi}_0(k)|^2 dk.$$

Using these expressions, one can verify that asymptotically, the invariant uncertainty product (28) does not depend on time, but it goes to the constant limit value proportional to x_c^2,

$$\tilde{\Delta}_\infty = x_c^2[\langle k^2\rangle(1 - \omega^2) - \langle k(\infty)\rangle^2]. \quad (53)$$

This formula is a generalization of the special case considered at the end of Section 2 to the case of arbitrary

(nonabsorbing) mirrors and arbitrary (narrow) initial packets. Only in the case of $\zeta(k) = \omega = 1$ the right-hand side of Eq. (53) turns into zero. But this is the case of free motion, when Δ preserves its initial value.

3.3. Momentum Transformation Coefficient

Using Eqs. (45)–(47), it is easy to show that the mean momentum transformation coefficient (21) can be made arbitrarily close to 1, provided one chooses a proper initial state. Suppose that the particle left some atomic trap passing inside a long planar waveguide of a width s. Then the initial coordinate wave function $\tilde{\psi}_0(y)$ has the form (for odd modes, $n = 1, 3, 5, \ldots$, for certainty)

$$\tilde{\psi}_0(y) = \begin{cases} \sqrt{(2/s)}e^{ik_0 y}\cos(n\pi y/s), & |y| < s/2, \\ 0, & |y| > s/2 \end{cases} \quad (54)$$

and the initial momentum distribution is the following function of the wave number k:

$$\mathcal{P}_0(k) = \frac{4\pi s n^2 \cos^2[s(k-k_0)/2]}{[(n\pi)^2 - s^2(k-k_0)^2]^2}, \quad (55)$$

$$\langle \hat{k}(0)\rangle = k_0, \quad \sigma_k(0) = (n\pi/s)^2.$$

For $k_0 = 0$ and $n \gg 1$, function (55) has high and sharp maxima at $k_n = \pm n\pi/s$ (the ratio $\mathcal{P}(k_n)/\mathcal{P}(0)$ equals $\pi^2 n^2/16$, whereas the width of the peak is of the order of π/s). Consequently, the main contributions to the integrals (46) and (47) are made from the region nearby k_n. Thus $\langle k^2\rangle \longrightarrow k_n^2$, $\langle k(\infty)\rangle \longrightarrow k_n$, and $\eta \longrightarrow 1$ as $n \longrightarrow \infty$. Explicitly, the asymptotical value of the mean momentum equals (for $k_0 = 0$)

$$\langle \hat{k}(\infty)\rangle = \frac{2}{\pi^2 n s}[(n\pi)^2 \mathrm{Si}(n\pi) - 2n\pi],$$

where

$$\mathrm{Si}(z) = \int_0^z \frac{\sin(t)}{t} dt.$$

For $n \gg 1$,

$$\mathrm{Si}(n\pi) = \frac{\pi}{2} + \frac{1}{n\pi} + \ldots, \quad n \quad \text{odd},$$

$$\tilde{k}(\infty) = 1 - \frac{2}{n\pi^2} + \ldots, \quad \eta_{\max} = 1 - \frac{4}{n\pi^2} + \ldots .$$

4. DISCUSSION

We have studied the influence of different factors on the effect of quantum deflection from atomic mirrors. This effect exists if the initial mean momentum in the direction perpendicular to the surface of the mirror is much less than the initial mean squared fluctuation of the momentum, $|p_0| < \hbar/s$, where s is the initial uncertainty in the position in the perpendicular direction (this uncertainty has an order of magnitude of the diameter of the atomic waveguide used to collimate the atomic beam). In this case, more than half (and even almost 100%, depending on the form of the initial packet) of the initial "internal" energy of quantum fluctuations can be transformed into the kinetic energy of the center of the wave packet associated with the particle. It is important that for narrow packets, localized initially sufficiently far from the mirror, and for totally (or almost totally) reflecting mirrors, the concrete form of the effective reflection potential does not influence the asymptotical (and averaged over fast oscillations) distributions of the coordinates and momenta related to the translational degrees of freedom of the particle. A possible quantum impurity also does not influence the effect, at least for initial Gaussian states.

The effect of deflection is accompanied (for narrow initial packets) by a significant increase (by many orders of magnitude) of the invariant uncertainty product, which characterizes the volume occupied by the packet in the phase space. The asymptotical (or maximal) value of this product is proportional to the square of the initial distance from the mirror. Also, the marginal distribution functions of the coordinate and momentum, as well as the Wigner quasiprobability distribution, exhibit strong oscillations in this case, indicating the "nonclassical" nature of the emerging quantum state describing the motion of the center of mass of the particle.

Now let us discuss the conditions under which the effect of quantum deflection can be observed in experiments with ultracold atoms. Suppose that an atom has the initial velocity in the direction almost parallel to the surface of some mirror. In this case, the expressions derived in the preceding sections describe the motion in the direction perpendicular to the surface. For the further estimations we assume that $p_0 = 0$. In order to see a significant deflection, the initial mean velocity in the direction parallel to the surface, $v_\parallel$, must be of the same order of magnitude as the asymptotical transverse velocity, $v_\infty \approx \hbar/(2ms)$. Taking $s = 10^{-6}$ cm, we obtain $v_\infty \sim 2$ cm/s for Cs atoms and $v_\infty \sim 2$ m/s for hydrogen atoms. According to the results of Section 2, the mean velocity becomes close to the asymptotical value v_∞ for $\tau > 5$. Consequently, the "deflection time" can be evaluated as

$$t_d \approx 5\beta/b^2 = 5\beta(ms^2/\hbar) \approx 4msx_c/\hbar. \quad (56)$$

Taking the initial distance from the boundary $x_c = 1$ cm, which is a quite macroscopic parameter (in this case $\beta \sim 10^6$), we have $t_d \sim 1$ s for Cs atoms and $t_d \sim 0.01$ s for hydrogen atoms. During this time the atom will pass about $2x_c$ in the parallel direction and about x_c in the

perpendicular direction. So, the "quantum deflection" can be quite observable. The effect is rather impressive from the classical point of view: a particle passes in 1 cm from the wall, nonetheless, in the absence of any visible force, it "feels" the presence of the boundary and changes the direction of motion by 45° (or even more, if the initial parallel velocity is less than v_∞). For light atoms, from H to Be, one can increase the initial distance even to 10 cm.

However, since the deflection time is rather large in the atomic scale, the influence of gravity can be essential, because the vertical shift of the hydrogen atom by 1 cm changes its potential energy by 10^{-9} eV. One can partially overcome this difficulty, using the *vertical* boundary and directing the particle upwards (some kind of "atom fountain" [46]). Moreover, adjusting the initial velocity, one can achieve zero displacement in the vertical direction due to the force of gravity, and a significant displacement in the horizontal direction due to the "quantum repulsive force." For example, for atoms of ^{9}Be and the initial distance $x_c \approx 3$ cm, one has $t_d \sim 0.3$ s. Taking the initial vertical velocity $v_\parallel \approx 1.5$ m/s, in 0.3 s one shall discover the atom at the same horizontal level, but shifted (in average) to about 3 cm from the initial position, so that the center of the distribution will be in 6 cm from the boundary (the maximal vertical displacement will be about 10 cm). The same result holds for the hydrogen atoms, if the initial transverse position uncertainty is $s = 0.1$ μm. Unfortunately, increasing parameter s diminishes the asymptotical transverse mean velocity and increases the time t_d, which makes difficult the compensation of the gravity force. The influence of mass is even more essential: since the change of the potential energy $U_g \sim mgx_c$ (here g is the free fall acceleration due to the gravity) is proportional to mass, while the kinetic energy of quantum fluctuations $E_k \sim \hbar^2/(ms^2)$ (at which expense the atom acquires the transverse velocity of the center of mass) is inversely proportional to mass, the parameter $\kappa = U_g/E_k \sim gm^2s^2x_c/\hbar^2$ is proportional to m^2. To observe the effect of deflection one needs $\kappa < 1$. Therefore, for heavy atoms, such as Cs, it is necessary to diminish the product s^2x_c by two orders of magnitude, comparing with atoms like Be. Nonetheless, we hope that the effect of quantum deflection can be observed for light ultracold atoms.

To verify the effect, one could put a detector at different positions at the same horizontal level and measure the probability of detecting the particles as a function of the distance to the boundary. The theoretical curve (Fig. 3) exhibits a strong asymmetry with respect to the initial particle position x_c. Moreover, if the space resolution of the detector could be made less than the initial transverse position uncertainty s, then the oscillations of the probability density due to the quantum interference effects could be discovered.

Note that the effect discussed does not depend on the internal state of the atom, since it is related only to the translational motion of its center of mass. Therefore, it must exist for any kind of atomic mirrors, including evanescent wave atomic mirrors [10–14] and magnetic mirrors [15, 16]. Moreover, for the velocities required, the De Broglie wavelength has the same order of magnitude as the initial transverse uncertainty s, so it is much greater than the interatomic distances in solids. Therefore the atomic structure of the solid surface seems to be unessential (because there are no "direct" collisions between the atom involved and the atoms of the boundary), and any surface seems to be close to an ideal impenetrable boundary.

On the other hand, the details of the effect (e.g., probability distributions in the coordinate, momentum, and phase spaces) depend essentially on the initial shape of the wave packet describing "external" (i.e., related to the motion of the center of mass of the atom) degrees of freedom, being significantly different for "narrow" and "wide" packets. In principle, these details could be also verified experimentally, since the methods of generating arbitrary quantum states of the center of mass motion have been proposed recently [47].

Several interesting problems emerge in connection with our study.

(1) In the real experiments with cold atoms, if the atom striking the mirror is not reflected from it, hardly it will pass through the glass ground of, say, an evanescent mirror. Sooner, it will be absorbed by this ground. Therefore, the case of *absorbing* atomic mirrors seems to be interesting for further studies.

(2) We have shown that in the presence of the wall, the mean momentum of a particle is changed at the expense of the energy of internal quantum fluctuations, due to some effective nonlocal quantum interaction. But the ideal wall is the limiting case of repulsive potentials. Therefore, one may suppose that the initial form of the wave packet could be important in the processes of collisions between ultracold particles, when absolute values of their initial mean momenta are less or comparable with the square roots of the momenta dispersions (this is a further step to the true quantum domain, compared with the cases studied until now [7]). As a result of a distortion of the shapes of the particle wave packets during the collision, the absolute values of the *mean momenta* will not be conserved. In this sense, the collisions between ultracold particles turn out inelastic, as far as the initial states are not idealized plane waves, but wave packets of finite spatial extensions. This effect could be important for the physics of ultracold atoms (in this connection see also, e.g., recent papers [48]).

(3) We have considered the effect of quantum deflection of *single atoms*. However, due to the fast development of the theory and experiments with beams of atoms in the state of the Bose–Einstein condensate (atomic lasers), it would be interesting to see, whether

the effect of quantum deflection exists for such beams. In this case we have to deal with *nonlinear* modifications of the Schrödinger equation, such as

$$i\hbar\frac{\partial\psi}{\partial t} = \frac{\hbar^2}{2m}\left(-\frac{1}{2}\Delta\psi + \Omega\{\psi\}\psi\right),$$

where $\Omega\{\psi\}$ is some nonlinear functional. If $\Omega\{\psi\} = f(|\psi|^2)$, where $f(z)$ is more or less arbitrary function, satisfying the condition $f(0) = 0$ (a special case $f(z) = az$ corresponds to the Gross–Pitaevsky equation, frequently used in the theory of Bose–Einstein condensates), then the Ehrenfest equations for the mean values of the coordinate and momentum have formally the same form (3) as in the one-particle case. However, the solutions $\psi(x, t)$ are different. Therefore, it is not clear whether the "quantum repulsive force" will be strong enough to cause a significant deflection of the beam or not. Actually, the treatment of the effect in Sections 2 and 3 was based essentially on the superposition principle for the De Broglie's waves, i.e., on the linearity of quantum mechanics. In the nonlinear case the situation could be quite different. For example, nonlinear equations admit *nonspreading beams* in the free space. In such a case, one could suppose that no partial plane wave would reach the boundary to be reflected from it, consequently, no quantum deflection would occur. Indeed, it was shown in [49] that the 5-parameter family of the *homogeneous* generalizations of the Schrödinger equation [50–53] contains a subfamily admitting the *finite-length* soliton solutions in the form (in the single space dimension, for simplicity)

$$\psi(x, t) = \{\cos[\gamma(x - kt)]\}^{1+\delta} e^{i(kx - \omega t)}, \qquad (57)$$

if $|\gamma(x - kt)| < \pi/2$, whereas $\psi(x, t) \equiv 0$ if $|\gamma(x - kt)| \geq \pi/2$ and $\delta > 0$. These solutions are continuous and have continuous first derivatives. The simplest representative of the subfamily discussed is the Kibble equation [54] with $\Omega\{\psi\} = \chi|\nabla\psi|^2/|\psi|^2$, $\chi > 0$, when $\delta = 2\chi/(1 - 2\chi)$ and $\gamma^2 = [2\omega - k^2(1 + 2\chi)](1 - 2\chi)$. Since solutions (57) are equal to zero identically outside some finite domain in the space, it is evident that any potential outside this domain does not effect these solutions. Studying a possibility of quantum deflection from mirrors for other kinds of nonlinear modifications of the Schrödinger equation, one could establish new bounds on the coefficients of these equations.

ACKNOWLEDGMENTS

The authors are grateful to the Brazilian agencies FAPESP and CNPq for the support.

REFERENCES

1. Adams, C.S., Sigel, M., and Mlynek, J., 1994, *Phys. Rep.*, **240**, 143.
2. Metcalf, H. and van der Straten, P., 1994, *Phys. Rep.*, **244**, 204.
3. Dowling, J.P. and Gea-Banacloche, J., 1996, *Adv. At., Mol., Opt. Phys.*, **37**, 1.
4. Baldwin, K.G.H., 1996, *Austr. J. Phys.*, **49**, 855.
5. Bigelow, N.P., Chalupczak, W., Ejnisman, R., *et al.*, 1998, *Acta Phys. Pol. A*, **93**, 11.
6. Cohen-Tannoudji, C.N., 1998, *Rev. Mod. Phys.*, **70**, 707.
7. Weiner, J., Bagnato, V.S., Zilio, S., and Julienne, P.S., 1999, *Rev. Mod. Phys.*, **71**, 1.
8. Wieman, C.E., Pritchard, D.E., and Wineland, D.J., 1999, *Rev. Mod. Phys.*, **71**, S253.
9. Balykin, V.I., 1999, *Adv. At., Mol., Opt. Phys.*, **41**, 181.
10. Cook, R. and Hill, R., 1982, *Opt. Commun.*, **43**, 258.
11. Balykin, V.I., Letokhov, V.S., Ovchinnikov, Y.B., and Sidorov, A.I., 1988, *Phys. Rev. Lett.*, **60**, 2137.
12. Westbrook, N., Westbrook, C.I., Landragin, A., *et al.*, 1998, *Phys. Scr. T*, **78**, 7.
13. Henkel, C., Wallis, H., Westbrook, N., *et al.*, 1999, *Appl. Phys. B*, **69**, 277.
14. Grimm, R., Weidemuller, M., and Ovchinnikov, Y.B., 2000, *Adv. At., Mol., Opt. Phys.*, **42**, 95.
15. Hinds, E.A. and Hughes, I.G., 1999, *J. Phys. D*, **32**, R119.
16. Poulsen, U.V. and Mølmer, K., 2000, *Eur. Phys. J. D*, **11**, 151.
17. Segev, B., Côté, R., and Raizen, M.G., 1997, *Phys. Rev. A*, **56**, R3350; Côté, R., Segev, B., and Raizen, M.G., 1998, *Phys. Rev. A*, **58**, 3999.
18. Dodonov, V.V. and Andreata, M.A., 2000, *Phys. Lett. A*, **275**, 173.
19. Doncheski, M.A. and Robinett, R.W., 1999, *Eur. J. Phys.*, **20**, 29.
20. Ol'shanii, M.A., Ovchinnikov, Yu.B., and Letokhov, V.S., 1993, *Opt. Commun.*, **98**, 77.
21. Marksteiner, S., Savage, C.M., Zoller, P., and Rolston, S.L., 1994, *Phys. Rev. A*, **50**, 2680.
22. Subbotin, M.V., Balykin, V.I., Laryushin, D.V., and Letokhov, V.S., 1997, *Opt. Commun.*, **139**, 107.
23. Dodonov, V.V., Malkin, I.A., and Man'ko, V.I., 1974, *Physica* (Amsterdam), **72**, 597.
24. 1953, *Higher Transcendental Functions (Bateman Manuscript Project)*, Erdélyi, A., Ed. (New York: McGraw-Hill), vol. 2.
25. Gradshtein, I.S. and Ryzhik, I.M., 1994, *Tables of Integrals, Series and Products* (New York: Academic).
26. Bonci, L., Roncaglia, R., West, B.J., and Grigolini, P., 1992, *Phys. Rev. A*, **45**, 8490.
27. Schrödinger, E., 1930, *Sitzungsber. K. Preuss. Akad. Wiss., Phys. Math. Kl.*, **24**, 296; Robertson, H.P., 1930, *Phys. Rev.*, **35**, 667.
28. Dodonov, V.V., Kurmyshev, E.V., and Man'ko, V.I., 1980, *Phys. Lett. A*, **79**, 150.
29. Dodonov, V.V. and Man'ko, V.I., 1989, *Invariants and the Evolution of Nonstationary Quantum Systems* (Proceedings of Lebedev Physics Institute, vol. 183), Markov, M.A., Ed. (New York: Nova Sci.).
30. Trifonov, D.A., 2000, *J. Opt. Soc. Am. A*, **17**, 2486.
31. Dodonov, V.V. and Man'ko, V.I., 1985, *Group Theoretical Methods in Physics: Proceedings of the Second International Seminar*, 1982, Zvenigorod, Markov, M.A.,

Man'ko, V.I., and Shabad, A.E., Eds. (London: Harwood Academic), vol. 1, p. 591.

32. Dodonov, V.V., 2000, *J. Phys. A*, **33**, 7721; Dodonov, V.V. and Man'ko, O.V., 2000, *J. Opt. Soc. Am. A*, **17**, 2403.
33. Dragt, A.J., Neri, F., and Rangarajan, G., 1992, *Phys. Rev. A*, **45**, 2572.
34. Rivera, A.L., Atakishiyev, N.M., Chumakov, S.M., and Wolf, K.B., 1997, *Phys. Rev. A*, **55**, 876.
35. Heller, E., 1991, *Chaos and Quantum Physics*, Giannoni, M.-J., Voros, A., and Zinn-Justin, J., Eds. (Amsterdam: Elsevier), p. 547.
36. Dodonov, V.V., Klimov, A.B., and Man'ko, V.I., 1993, *Squeezed and Correlated States of Quantum Systems* (Proceedings of Lebedev Physics Institute, vol. 205), Markov, M.A., Ed. (New York: Nova Sci.), p. 61.
37. Dodonov, V.V. and Man'ko, V.I., 1994, *Modern Nonlinear Optics* (Advances in Chemical Physics Series, vol. 85), Evans, M. and Kielich, S., Eds. (New York: Wiley), part 3, p. 499.
38. Yuen, H.P., 1983, *Phys. Rev. Lett.*, **51**, 719; Storey, P., Sleator, T., Collett, M., and Walls, D., 1994, *Phys. Rev. A*, **49**, 2322; Walls, D., 1996, *Austr. J. Phys.*, **49**, 715.
39. Clark, T.E., Menikoff, R., and Sharp, D.H., 1980, *Phys. Rev. D*, **22**, 3012.
40. Akhundova, E.A., Dodonov, V.V., and Man'ko, V.I., 1985, *J. Phys. A*, **18**, 467.
41. Cheng, B.K., 1990, *J. Phys. A*, **23**, 5807.
42. Gea-Banacloche, J., 2000, *Opt. Commun.*, **179**, 117.
43. Landau, L.D. and Lifshitz, E.M., 1977, *Quantum Mechanics: Non-Relativistic Theory*, 3rd ed. (Oxford: Pergamon).
44. Faddeev, L.D., 1958, *Dokl. Akad. Nauk SSSR*, **121**, 63 [1958, *Sov. Phys. Dokl.*, **3**, 747].
45. Lamb, G.L., Jr., 1980, *Elements of Soliton Theory* (New York: Wiley).
46. Kasevich, M.A., Riis, E., Chu, S., and De Voe, R.G., 1990, *Phys. Rev. Lett.*, **63**, 612.
47. Olshanii, M., Dekker, N., Herzog, C., and Prentiss, M., 2000, *Phys. Rev. A*, **62**, 033612.
48. Kälbermann, G., 1999, *Phys. Rev. A*, **60**, 2573; 2001, *J. Phys. A*, **34**, 3841.
49. Caparelli, E.C., Dodonov, V.V., and Mizrahi, S.S., 1998, *Phys. Scr.*, **58**, 417.
50. Gradov, O.M. and Stenflo, L., 1982, *Phys. Fluids*, **25**, 983; Malomed, B.A. and Stenflo, L., 1991, *J. Phys. A*, **24**, L1149.
51. Sabatier, P.C., 1990, *Inverse Probl.*, **6**, L47; Auberson, G. and Sabatier, P.C., 1994, *J. Math. Phys.*, **35**, 4028.
52. Doebner, H.-D. and Goldin, G., 1992, *Phys. Lett. A*, **162**, 397; Doebner, H.-D. and Goldin, G., 1994, *J. Phys. A*, **27**, 1771.
53. Dodonov, V.V. and Mizrahi, S.S., 1993, *J. Phys. A*, **26**, 7163; Dodonov, V.V. and Mizrahi, S.S., 1995, *Ann. Phys.* (New York), **237**, 226.
54. Kibble, T., 1978, *Commun. Math. Phys.*, **64**, 73.